

Tunable, monochromatic x rays using the internal beam of a betatron

V. V. Kaplin^{a)} and S. R. Uglov

Nuclear Physics Institute, Tomsk Polytechnic University, P. O. Box 25, Tomsk 634050, Russia

O. F. Bulaev, V. J. Goncharov, and A. A. Voronin

Institute of Introscopy, Savinikh st. 3, Tomsk 634034, Russia

M. A. Piestrup^{b)} and C. K. Gary

Adelphi Technology, Inc., 2181 Park Boulevard, Palo Alto, California 94306

N. N. Nasonov

Laboratory of Radiation Physics, Belgorod State University, Studencheskaja 12, 308007 Belgorod, Russia

M. K. Fuller

OSMIC Incorporated, 201 Hoffman Avenue, Suite 6, Monterey, California 93940

Tunable, monochromatic x rays from thin radiators mounted inside a betatron have been observed. Parametric x-ray radiation (PXR) was generated by 33-MeV electrons passing multiple times through three radiators: a 43- μm -thick Si crystal, a 400- μm -thick graphite crystal, or a 310-layered-pair (W and B_4C , $d=14.86 \text{ \AA}$) multilayer. The pulse-height spectrum of the radiation (5 to 30 keV) was obtained and was tuned by rocking the crystal or multilayer relative to the electron-beam direction. The experimental results appear to follow theoretical predictions for PXR emission with some modification required for the curved trajectory of the electrons.

Recycling electrons through thin targets can enable the production of intense, monochromatic x rays from cyclical accelerators using periodic media and crystalline targets.^{1,2} To make these sources useful for industrial and medical imaging applications, we wish to use modest electron-beam energies generated by inexpensive sources such as the modern betatron.³⁻⁷ The aim of the present work is to demonstrate feasibility by observing the pulse-height spectrum from multiple passes of electrons incident on either crystal or multilayer radiators mounted inside a betatron.

The radiators used here all generated parametric x rays.^{8,9} This emission occurs when an electron passes through a crystal, or a multilayer,¹⁰ at an angle θ_0 with respect to a set of the atomic planes, or multilayer planes. Parametric x-ray radiation (PXR) is emitted at $\theta_D=2\theta_0$ with respect to the electron path due to the Bragg scattering of virtual photons from the electron.⁸ The radiation is defined by the coherent superposition of the waves emitted from the atoms of the crystal or multilayer planes. The angular and spectral distributions of PXR are narrow.¹¹

Three radiators were used: a 43- μm -thick Si crystal, a 400- μm -thick graphite crystal, or a 310-layered-pair (W and B_4C , $d=14.86 \text{ \AA}$) multilayer (x-ray mirror from OSMIC Inc.). The experimental apparatus is shown in Fig. 1. We used the 35-MeV Research Institute of Introscopy betatron, model number B-35. Electrons are injected at 60 keV into the ceramic toroid of the betatron (2) and accelerated to the desired energy to a stable orbit of $R_0=245 \text{ mm}$ by means of a rising magnetic field. The electrons are then dumped on an internal target (3) by an additional magnetic field of 30- μs

duration. This change in magnetic field alters the betatron condition, moving the equilibrium orbit of the electron inwards so that the electrons strike the edge of the radiator (3). The electron beam then recirculates, passing through the thin radiator many times, resulting in increased emission but also increased electron-beam emittance.

The repetition rate of the betatron was 50 Hz. The divergence of the electron beam was less than 0.3 mrad, and the electron energy spread was 0.5%.

The radiators were supported by a set of thin wires that could mechanically rotate them. PXR was emitted from the

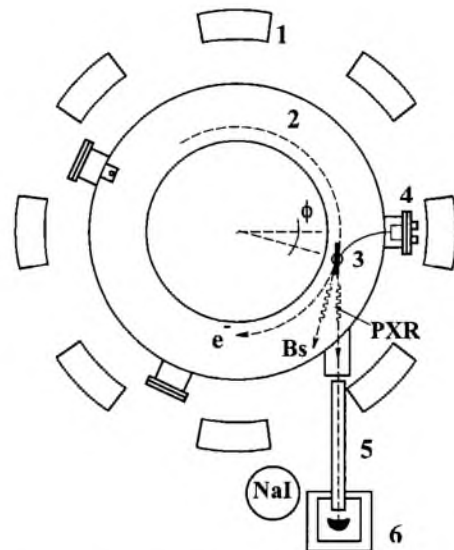


FIG. 1. Experimental arrangement: 1—betatron magnet; 2—betatron toroid; 3—internal target; 4—goniometer; 5—vacuum pipe; and 6—CdTe x-ray detector.

^{a)}Electronic mail: kaplin@npi.tpu.ru

^{b)}Electronic mail: melpie@adelphitech.com

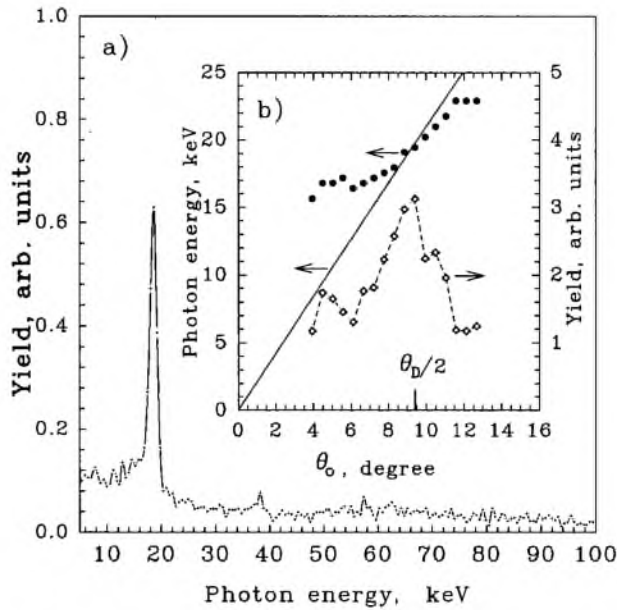


FIG. 2. (a) Spectrum of PXR generated by 33-MeV electrons in 43- μm (220) Si crystal at its symmetrical orientation $\theta_0 = \theta_D/2 = 9.4^\circ$ in the Laue geometry for x-ray production. (b) Spectral peak position of the PXR as a function of θ_0 . The solid curve is the theoretical dependence of the spectral peak position [Eq. (1)]. The PXR yield as a function of θ_0 is marked by diamonds.

radiators passed through a 12- μm Kapton® (polyimide) window and detected by a CdTe detector (6) (Model 100 TD, AMPTEK Inc.). The detector was placed at the angle θ_D ranges of about 19° – 20° and 9° – 11° with respect to the electron-beam direction in order to observe PXR with photon energy of around 20 keV in the case of the Si and pyrolytic graphite crystals, respectively. The detector was either 148 cm or 100 cm from the target with the PXR photon path in the air of 110 cm or 62 cm, respectively. The detector aperture was 4 mm², the energy resolution at the ⁶³Zn line (8.1 keV) was about 10%. To minimize the absorption of the generated PXR, we used a vacuum pipe (5) placed between toroid window and detector (6).

The Si crystal was mounted in an azimuthal position $\phi = 19^\circ$, giving the emission angle $\theta_D = 19^\circ$ in the Laue geometry. The PXR spectra measured at the angle $\theta_0 = 9.4^\circ$ between the electron-beam direction and the (220) crystallographic planes of the 43- μm -thick Si crystal with vertical and horizontal dimensions of 7.0 mm and 5.0 mm, respectively, are shown in Fig. 2(a). The result demonstrates the bright spectral peak with the peak-height/background-level (P/B) ratio (spectral-peak contrast) of about 9 and with the full width at half maximum (FWHM) of about 1.5 keV.

The peak changes its position and intensity by rocking the crystal in angle relative to the electron (by rotating the crystal around vertical axis). The expected theoretical dependence of spectral peak position is given by:^{8,9,11}

$$E_{\gamma\text{PXR}} = \frac{2\pi n\hbar \sin \theta_0}{d(1 - \cos \theta_D + 1/2\gamma^2)}, \quad (1)$$

where d is the crystal plane spacing, $\theta_0 = \theta_B + \Delta\theta_0$ is an angle between the electron beam and the set of crystal planes, θ_D is a detector disposition angle (the angle of emis-

sion with respect to the electron-beam direction), θ_B is the optimum Bragg angle, and γ is the relativistic factor of the electrons.

From the virtual-photon approach, the FWHM of the PXR the distribution will be $\Delta\theta_\gamma \approx 5\theta_{\text{ph}}$, where $\theta_{\text{ph}} = [\gamma^{-2} + (\hbar\omega_p/E_\gamma)^2]^{1/2}$, ω_p is the plasma frequency of the medium. But if the electron energy is modest, the FWHM will be about $\Delta\theta_\gamma = 5\gamma^{-1}$. The angular distribution of PXR for the thin crystal has the maximum of the angles θ_{ph} (or γ^{-1}) with respect to the radiation cone axis.

The measured dependencies of the PXR peak position and yield from the crystal orientation θ_0 are shown in Fig. 2(b) by the points and diamonds, respectively. For comparison, the solid curve is the theoretical dependence of the peak position as given by Eq. (1). As can be seen, the theoretical curve deviates from the experimental at the extremes of the rotation. This may be due to the fact that the electron trajectory is circular and not straight as assumed in Eq. (1).

The FWHM of PXR yield in a collimated detector is two times less than the FWHM of PXR angular distribution. That is similar to the case of the rocking-curve method used in diffraction of real photons in the crystals. The value of the FWHM of PXR yield (rocking curve) measured is greater than that estimated herein. This may be due to the increased emittance due to the recycling process.³

The 400- μm -thick pyrolytic graphite (PG) crystal was mounted in the azimuthal position $\phi = 8.6^\circ$ in the Bragg geometry for PXR generation. The spectra of PXR was measured at $\theta_0 = 4^\circ$, 4.7° , and 2.5° [curves 1–3 in Fig. 3(a)] between the 33-MeV electron-beam direction and (200) PG crystallographic planes. The central peak was obtained at symmetrical orientation of the PG crystal and gives a P/B ratio of about 10. The FWHM of the spectral peak is about 3.75 keV. This is larger than that observed in the case of the Si crystal due to the mosaicity of the PG crystal.¹²

Figure 3(b) shows the orientational dependencies of PXR yield (diamonds) and the spectral-peak position (points). The FWHM of yield dependence measured is in good agreement with the theoretical value $\Delta\theta_\gamma/2$ of the rocking-curve width. The solid line shows the theoretical dependence of the PXR spectral peak position calculated according to formula (1).

PXR was also generated from a multilayer using moderate-energy electrons. Previously, we observed x-ray emission from a similar multilayer using 500-MeV electrons.¹⁰ Multilayers consist of a large number, N , of alternating nanolayers of different materials and are good reflectors of x rays.¹³ Our multilayer consisting of W and B₄C layers with spacing $d = 14.86 \text{ \AA}$ and $N = 310$ layer pairs was deposited on a 250- μm Si substrate. The vertical and horizontal dimensions were $3.5 \times 1.0 \text{ mm}^2$. After etching the Si substrate to 15 μm , the radiator became slightly curved, which may have broadened the spectral line.

The multilayer was set at the azimuthal position of $\theta_D = 6^\circ$. The spectra of PXR generated by 33-MeV electrons in the multilayer at the angle $\theta_0 = 1.75^\circ$, 3.25° , 4.75° is shown in Fig. 4(a). As can be seen, the spectral peak (curve 2) at the photon energy of 8 keV was observed close to the symmetrical target position, $\theta_0 = 3.25^\circ$. The FWHM of spectral peak is about 2 keV. The solid curve shows the spectrum measured

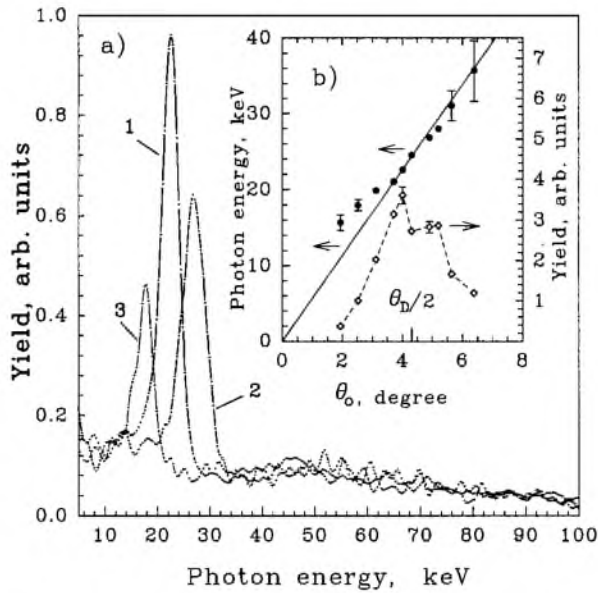


FIG. 3. (a) Spectra of PXR generated by 33-MeV electrons in a (200) pyrolytic graphite crystal with height, width, and thickness of 7, 4, and 0.4 mm at the crystal orientations $\theta_0 = 4^\circ, 4.7^\circ, 2.5^\circ$, curves 2 and 3, in Bragg geometry for x-ray generation. (b) The spectral-peak position and the yield of PXR generated by 33-MeV electrons in the same PG crystal marked by points and diamonds, respectively.

without the vacuum pipe (5) resulting in the PXR spectral peak being absorbed.

The measured dependencies of spectral peak position and radiation yield as a function of the rocking angle $\Delta\theta_0$ are shown in Fig. 4(b) by points and diamonds, respectively. The energy of generated photons decreases for decreasing angle θ_0 in accordance with the theory.⁹

In conclusion, moderate energy betatron electrons can generate monochromatic and directional x rays from crystalline and multilayer targets. Both the single and mosaic crystals are excellent candidates for radiators because the estimated PXR flux is high (e.g., 0.04 photons per 33-MeV electron per str for 5-mm-thick PG at $\theta_D = 10^\circ$). Multilayers can also be used for generation of PXR using electrons at energies much lower than previously used.¹⁰ Such a target is very promising because the estimated flux is also high (e.g., the flux for 8-keV x rays using 33-MeV electrons is 0.03 photons/electron/str. The effect of electron recirculation through the target, which is possible at the thickness of the targets used, does not degrade the monochromaticity and directionality of the PXR generated, although the scattering of electrons recycling and their energy losses in the target may cause an increase in the emittance.

This work was supported by the Russian Foundation of Basic Research and by the United States National Institute for Health under the Small Business Innovation Research

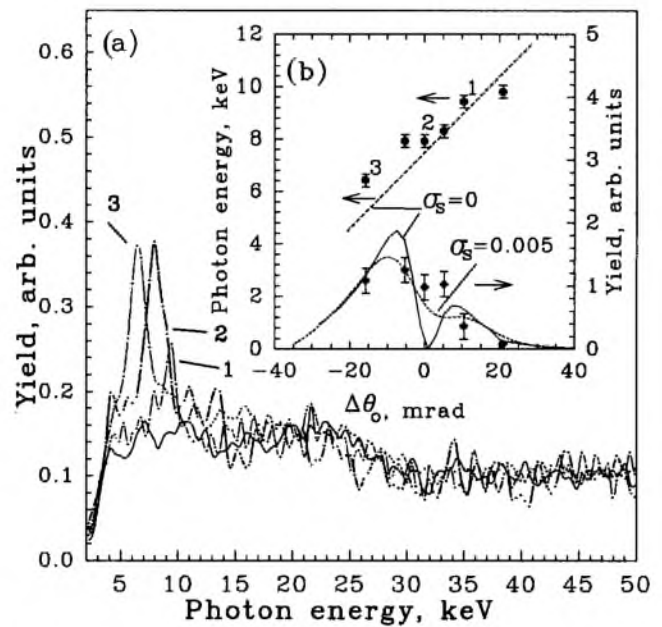


FIG. 4. (a) Spectrum of PXR generated by 33-MeV electrons in a $3.5 \times 1 \times 0.015$ mm³ x-ray mirror at its orientations $\theta_0 = 1.75^\circ, 3.25^\circ$, and 4.75° in Bragg geometry with $\theta_D = 6^\circ$, curves 1–3, respectively. Solid curve shows the spectrum measured without a vacuum pipe. (b) The spectral-peak position and PXR yield as a function of the rocking angle $\Delta\theta_0$ are marked by points and diamonds, respectively. Solid curves show theoretical dependencies.

(SBIR) program (Grant Nos. 1-R43-RR11647-02 and 1-R43 CA86545-01).

- ¹M. Y. Andreyashkin, V. V. Kaplin, M. A. Piestrup, S. R. Uglov, and V. N. Zabaev, *Appl. Phys. Lett.* **72**, 1385 (1998).
- ²M. A. Piestrup, L. W. Lombardo, J. T. Cremer, G. A. Retzlaff, R. M. Silzer, D. M. Skopik, and V. V. Kaplin, *Rev. Sci. Instrum.* **69**, 2223 (1998).
- ³V. V. Kaplin, L. Lombardo, A. A. Mihal'chuk, M. A. Piestrup, and S. R. Uglov, *Nucl. Instrum. Methods Phys. Res. B* **145**, 244 (1998).
- ⁴V. V. Kaplin, S. R. Uglov, O. F. Bulaev, V. J. Goncharov, M. A. Piestrup, and C. K. Gary, *Nucl. Instrum. Methods Phys. Res. B* **173**, 3 (2001).
- ⁵M. A. Piestrup, X. Wu, V. V. Kaplin, S. R. Uglov, J. T. Cremer, D. W. Rule, and R. B. Frioito, *Rev. Sci. Instrum.* **72**, 2159 (2001).
- ⁶M. A. Piestrup, M. W. Powell, J. T. Cremer, L. W. Lombardo, V. V. Kaplin, A. A. Mihal'chuk, S. R. Uglov, V. N. Zabaev, D. M. Skopik, R. M. Silzer, and G. A. Retzlaff, *Proc. SPIE* **3331**, 450 (1998).
- ⁷V. V. Kaplin, S. R. Uglov, O. F. Bulaev, V. J. Goncharov, M. A. Piestrup, and C. K. Gary, *Rev. Sci. Instrum.* **73**, 63 (2002).
- ⁸M. I. Ter-Mikaelian, *High Energy Electromagnetic Processes in Condensed Media* (Wiley, New York, 1972).
- ⁹N. N. Nasonov, M. A. Piestrup, C. K. Gary, V. V. Kaplin, and S. R. Uglov (unpublished).
- ¹⁰V. V. Kaplin, S. R. Uglov, N. V. Zabaev, M. A. Piestrup, C. K. Gary, N. N. Nasonov, and M. K. Fuller, *Appl. Phys. Lett.* **76**, 3647 (2000).
- ¹¹K.-H. Brenzinger, B. Limburg, H. Backe, S. Dambach, H. Euteneuer, F. Hagenbuck, C. Herberg, K. H. Kaiser, O. Kettig, G. Kube, W. Lauth, H. Schope, and T. Walcher, *Phys. Rev. Lett.* **79**, 2462 (1997).
- ¹²R. B. Fiorito, D. W. Rule, X. K. Maruyama, K. DiNova, M. J. Osborne, S. Evertson, D. Snyder, H. Rietdyk, M. A. Piestrup, and A. H. Ho, *Phys. Rev.* **71**, 704 (1993).
- ¹³T. W. Barbee, Jr., *Opt. Eng.* **25**, 893 (1986).